PAPER

Probing Lattice Vibrations at SiO$_2$/Si Surface and Interface with Nanometer Resolution[*]

To cite this article: Yue-Hui Li *et al* 2019 *Chinese Phys. Lett.* **36** 026801

View the article online for updates and enhancements.

中国物理快报
Chinese Physics Letters

CLICK HERE
for our
Express Letters

Probing Lattice Vibrations at SiO₂/Si Surface and Interface with Nanometer Resolution [*]

Yue-Hui Li(李跃辉)[1,2†], Mei Wu(武媚)[1,2†], Rui-Shi Qi(亓瑞时)[1], Ning Li(李宁)[1,2], Yuan-Wei Sun(孙元伟)[1,2],
Cheng-Long Shi(施成龙)[3], Xue-Tao Zhu(朱学涛)[4], Jian-Dong Guo(郭建东)[4],
Da-Peng Yu(俞大鹏)[2,5,6], Peng Gao(高鹏)[1,2,6**]

[1]International Center for Quantum Materials, Peking University, Beijing 100871
[2]Electron Microscopy Laboratory, School of Physics, Peking University, Beijing 100871
[3]Nion Company, 11511 NE 118Th Street, Kirkland, Washington State 98034, USA
[4]Beijing National Laboratory for Condensed Matter Physics and Institute of Physics,
Chinese Academy of Sciences, Beijing 100190
[5]Shenzhen Key Laboratory of Quantum Science and Engineering, Shenzhen 518055
[6]Collaborative Innovation Centre of Quantum Matter, Beijing 100871

Recent advances in monochromatic aberration corrected electron microscopy make it possible to detect the lattice vibrations with both high-energy resolution and high spatial resolution. Here, we use sub-10 meV electron energy loss spectroscopy to investigate the local vibrational properties of the SiO₂/Si surface and interface. The energy of the surface mode is thickness dependent, showing a blue shift as z-thickness (parallel to the fast electron beam) of SiO₂ film increases, while the energy of the bulk mode and the interface mode keeps constant. The intensity of the surface mode is well-described by a Bessel function of the second kind. The mechanism of the observed spatially dependent vibrational behavior is discussed and compared with dielectric response theory analysis. Our nanometer scale measurements provide useful information on the bonding conditions at the surface and interface.

Lattice vibrations play a major role in many physical properties of condensed matter.[1] At the surface and interface of solid materials, the change of atomic bonding is expected to alter the local vibrational behavior.[2] Therefore, exploring the localized vibrational properties is of significant importance, particularly in low dimensional systems.[3,4] The vibrational properties are commonly measured by high-resolution electron energy loss spectroscopy (EELS),[5,6] inelastic neutron scattering, infrared spectroscopy (IR),[7,8] and Raman spectroscopy,[9] which is typically at micrometer scale (unless assisted by a sharp metal tip[10] ∼20 nm). However, the recent advances of dedicated scanning transmission electron microscopes (STEMs) enable an electron probe with ∼10 meV in energy resolution and ∼0.1 nm in spatial resolution, allowing us to spatially map the lattice vibrations of a single nanostructure[11−21] and correlate property measurements with microstructures.

In this Letter, we use a ∼8 meV electron probe based on a Nion UltraSTEM™ 200 microscope to study the vibrational properties of the SiO₂/Si heterostructure, which is of importance for design of metal-oxide-semiconductor field effect transistors (MOSFETs)[22,23] with the device size down to tens of nanometer or lower.[24] We acquire three vibrational modes (i.e., TO₁ (∼60 meV), TO₂ (∼103 meV), TO₃ (∼130 meV–150 meV)) at different locations and capture the subtle changes of vibrational energy and intensity. We find that the vibration is highly spatially dependent and each optical mode splits into three branches (surface modes, bulk modes and interface modes). In particular, as the z-thickness decreases, the vibrational energy of surface modes shows a substantial red shift that is attributed to the enhanced coupling of upper and lower surface,[25] while the energy of bulk modes and interface modes remains unchanged. The intensity of the surface modes is well-described by a Bessel function of the second kind and the intensity of bulk mode is proportional to the slab thickness. Approaching the interface, the interface mode and guided mode cannot be distinguished due to their similar vibrational energy, but their total intensity decreases sharply. These results can be interpreted by a semiclassical relativistic local dielectric theory.[25−27] Our study reveals the vibrational behavior of SiO₂/Si with nanometer resolution and it provides useful insights into the fundamental electrical, optical and thermal properties of SiO₂/Si and thus may help to design better silicon-based electronic devices via surface and interface treatments.

A ∼6 meV zero-loss peak can be tuned up at 60 kV (Fig. S1 in the supplementary material). For a higher ratio of signal to noise, we significantly increase the acquisition time which only sacrifices the energy resolution slightly. Figure 1(a) shows three typical re-

gions to record the spectra, corresponding to surface (blue), mixture of bulk and surface (orange) and interface (cyan). Figure 1(b) shows the typical measured EELS with a probe beam located near the surface in vacuum side (cyan) and the vacuum far away from the specimen (orange). After background subtraction, the spectrum in Fig. 1(c) shows the three peaks, which are in agreement with previous IR spectroscopy and neutron scattering experiment.[28,29] The TO_1 mode is associated with Si–O–Si rocking motions, with bridging oxygen moving perpendicular to the Si–O–Si plane. The TO_2 mode is associated with transverse-optical stretching motions, with oxygen atoms moving along a line bisecting the Si–O–Si bond. The $TO_{3-surface}$ mode is associated with Si–O–Si antisymmetric stretching motion, with oxygen atoms moving along a line parallel to the Si-Si axis, as shown in Fig. 1(c).[29] The TO_{3-bulk} mode is associated with the network disorder.[30] The spatially resolved spectra show that these modes have different energies and intensities in different regions, indicating that the vibrational properties are sensitive to the surface and interface.
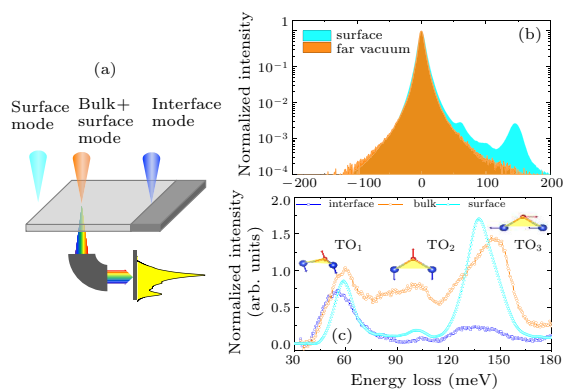

Fig. 1. Electron energy loss spectroscopy measurements of SiO_2 vibrational modes in a monochromatic aberration corrected electron microscope. (a) The spectra recorded from different regions represent different vibrational modes, surface mode (cyan), bulk mode+surface mode (orange), interface mode (blue). (b) Normalized spectra acquired with the electron beam located near the surface in vacuum side (cyan) and vacuum (orange) far away from specimen with energy resolution $\sim$8 meV. (c) Typical spectra after background subtraction. The insets show the schematic representation of the vibrational motions: TO_1 mode, rocking motion perpendicular to Si–O–Si plane. TO_2 mode, symmetric stretching motion along the bisector of the Si–O–Si bridging angle. TO_3 mode, antisymmetric stretching motion parallel to the Si-Si line between the two bridged cations. The orange region shows the Si–O–Si plane. The blue and red arrows indicate the atom motion directions.

We first investigate the surface effects on the vibrational spectra. Generally, the vibration changes at the surface due to the asymmetric bonding and the resonance condition is $\varepsilon_1 + \varepsilon_2 = 0$.[31] Figure 2(a) shows a high angle annular dark field (HAADF) image of amorphous SiO_2 (a-SiO_2) film on the Si substrate. In Fig. 2(b), the selected line profiles of spectra recorded from the vacuum to a-SiO_2 with 6.3 nm every step display that the peak of the TO_3 mode becomes broader

and shifts to higher energy in the a-SiO_2 region because the surface mode (originating from upper and lower surfaces) and the bulk mode are mixed together due to the small difference in energy. Figures 2(c) and 2(d) are the corresponding EELS mapping for experiments and simulations, respectively, in which the surface position is set to zero, and the negative (positive) distance denotes that the electron beam is in vacuum (a-SiO_2 film). The experiments and simulations both show that the TO_1 mode and TO_3 mode can spread over $\sim$600 nm in vacuum, while the TO_2 mode only concentrates near the surface. Using Gaussian functions (for details see Fig. S2 in the supplementary material) we decompose the signal in 120 meV–170 meV into two peaks, $TO_{3-surface}$ and TO_{3-bulk}, which represent the surface mode and bulk mode, respectively (the surface mode is 13 meV lower than the corresponding bulk mode). For the TO_1 mode, the energy difference between the bulk mode and the surface mode is subtle (about 3 meV), which is also consistent with the analysis of energy loss functions, while for the TO_2 mode, the significant broadening makes it hard to identify the peak positions in the SiO_2.

The energies of TO_1, TO_2, $TO_{3-surface}$, TO_{3-bulk} varying with position (for calculation details see Fig. S3 in the supplementary material) are plotted in Fig. 2(e). When the electron beam is positioned near the surface, the vibrational energies of TO_1, TO_2 and $TO_{3-surface}$ mode are 59 meV, 100 meV and 137 meV, compared to the calculation results: 60.5 meV, 100.4 meV and 139 meV (Fig. 2(d)). In agreement with previous reports,[30,32] the energy of TO_{3-bulk} is 150 meV. It should be noted that the intensity of TO_2 mode is too weak to be extracted from the tail of the TO_1 peak when the probe is positioned at 150 nm away from the SiO_2 surface.

Figure 2(f) shows the normalized intensity as a function of distance from the surface. The intensity of TO_{3-bulk} mode reaches 80% of its maximum value at 20 nm from the surface, while the $TO_{3-surface}$ intensity has the maximum value at the edge of surface and gradually decreases away from the edge (inset in Fig. 2(f)). At the edge, all of the top surface, bottom surface, and edge surface make significant contributions while far away from the edge only the top and bottom surface make contributions. The intensity distribution of the $TO_{3-surface}$ in the vacuum can be described by the relativity-modified dielectric response theory,[33] based on which the inelastic-scattering probability per unit energy loss E per unit length t for aloof-beam spectroscopy is

$$\frac{dP}{dEdt} = \frac{4}{\pi}\frac{\alpha}{\hbar c\beta^2}\mathrm{Im}\Big(\frac{-1}{\varepsilon_{SiO_2}(E)+1}\Big)K_0\Big(\frac{2bE}{\gamma\hbar c\beta}\Big), (1)$$

where t is the specimen thickness, $\alpha = 1/137$ is the fine-structure constant, $\hbar$ is the reduced Planck constant, $\beta = v/c$ is the ratio of beam velocity v to the speed of light c, $\gamma = (1-\beta^2)^{-1/2}$ is the Lorentz factor, and b is the impact parameter (the distance between the beam and the sample surface). The function K_0

is the zero-order modified Bessel function of the second kind. The vibrational intensity of the $TO_{1-surface}$ mode and the $TO_{3-surface}$ mode is very well described by Eq. (1). The blue and the red solid lines are the theoretical vibrational intensities derived from Eq. (1). The decay behavior can also roughly be fitted with the exponential function $I = I_0 \exp(-b/b_0)$.[11,34] With this approximation, the decay distance is fitted to be ~ 400 nm for $TO_{1-surface}$, ~ 350 nm for TO_2, and ~ 250 nm for $TO_{3-surface}$ (detailed data see Table 1 in the supplementary material).
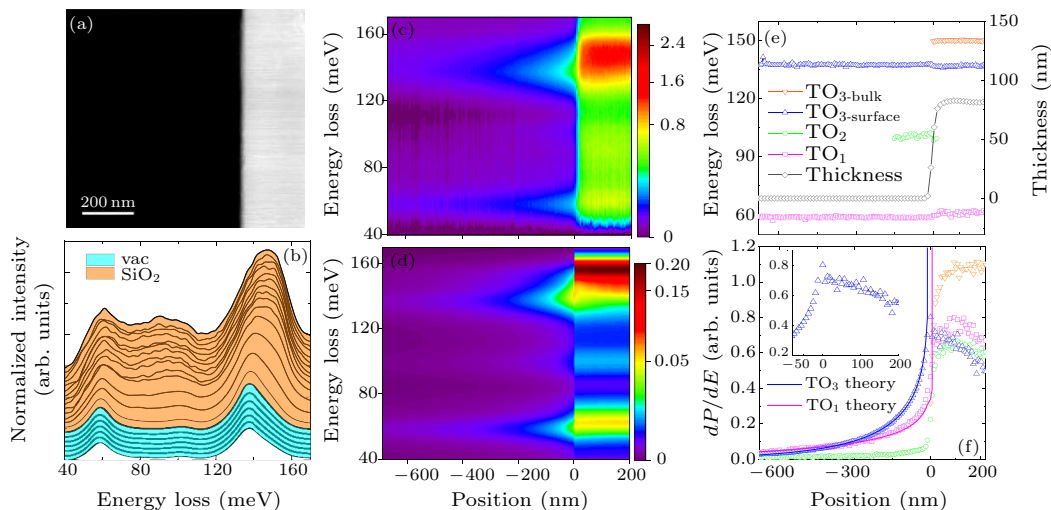

Fig. 2. Vibrational energy and intensity of SiO_2 surface. (a) HAADF image of vacuum/a-SiO_2/Si specimen viewed in cross-section. (b) Selected line profiles of the SiO_2 vibrational signal with 6.3 nm every stack. [(c), (d)] Two-dimensional plots of normalized intensity for experiment and simulation, respectively. The surface position is set to be zero, and negative distance denotes that the electron beam is in vacuum. Color bar represents the intensity. (e) The vibrational energies of different modes with different colors, and z-thickness (black) of SiO_2 slab is plotted as a function of the probe position. (f) Vibrational intensities are plotted as a function of the probe position. A solid line represents the theoretical calculation.
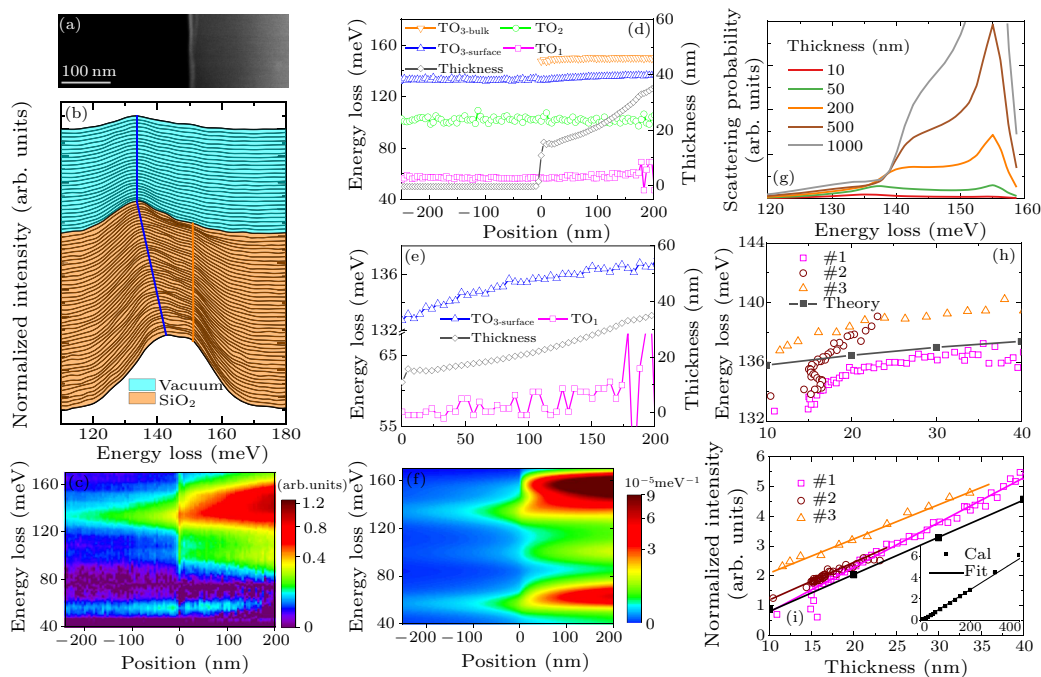

Fig. 3. Effects of film thickness on the vibrational energy and intensity. (a) HAADF image of vacuum/ a-SiO_2 viewed in cross section. (b) Selected line profile of the SiO_2 vibrational signal with 4.7 nm every stack. Two-dimensional plots of normalized intensity for (c) experiments and (f) simulations, respectively. The surface is set to be zero, and negative distance denotes that the probing beam is in vacuum. Color bar represents the normalized intensity. (d) Energy of vibrational modes (colored) and z-thickness (black) of SiO_2 slab as a function of the probe position. (e) Enlarged view of $TO_{3-surface}$ mode and TO_1 mode shows that the peak shift depends on the film thickness. (g) Energy loss function for different thicknesses. (h) Vibrational energy of the TO_3 mode as a function of z-thickness of SiO_2 slab. Colored data are recorded from different samples and the black points are calculated from the Kröger formula. (i) The intensity of TO_3 mode is plotted as a function of z-thickness of SiO_2 slab. The colored data represents different samples and a black point represents the calculation from the Kröger formula.

When the thickness of specimen is in the order of v/ω (where ω is the frequency of vibration and v is electron beam velocity) or less, the coupling of upper and lower surfaces would give rise to symmetric and asymmetric guided modes.[25] Figures 3(a) and 3(b) show an HAADF image and the selected line profile of SiO$_2$ spectra (4.7 nm every step) with non-uniform thickness, respectively. Figures 3(c) and 3(f) show the two-dimensional plots of normalized intensity for experiments and simulations, respectively. As the beam is moved from the edge to the inner, the energy of the TO$_{3-\text{surface}}$ mode (blue line) shows a significant blue shift while the energy of TO$_{1-\text{surface}}$ shows a smaller blue shift, as shown in Figs. 3(d) and 3(e). We attribute the blue shift to the reduced strength of coupling when z-thickness of SiO$_2$ slab increases (note that the sample thickness can be estimated from the low-loss EEL spectra). This energy shift behavior can be interpreted by the thickness dependent energy-loss functions plotted in Fig. 3(g) based on Kröger formula.[25] Specifically, the energy of the TO$_{3-\text{surface}}$ mode at the edge is 133 meV and increases to 136 meV distanced ~200 nm from the edge inside the film. In Fig. 3(h), three datasets from different specimens and calculations further confirm that the energy of the TO$_{3-\text{surface}}$ mode is very sensitive to SiO$_2$ thickness. The difference between the experiments and theory is likely to be due to the non-uniform specimen instead of ideal wedge-shaped films.

The vibrational intensity also depends on the thickness of SiO$_2$ film. Compared to the TO$_{3-\text{surface}}$ mode, the probability of TO$_{3-\text{bulk}}$ mode decreases more quickly as the z-thickness decreases. The normalized intensity of TO$_{3-\text{bulk}}$ mode is plotted as a function of SiO$_2$ slab thickness for the three datasets, which are all proportional to the slab thickness as we expect from the theoretical calculation (shown in inset).
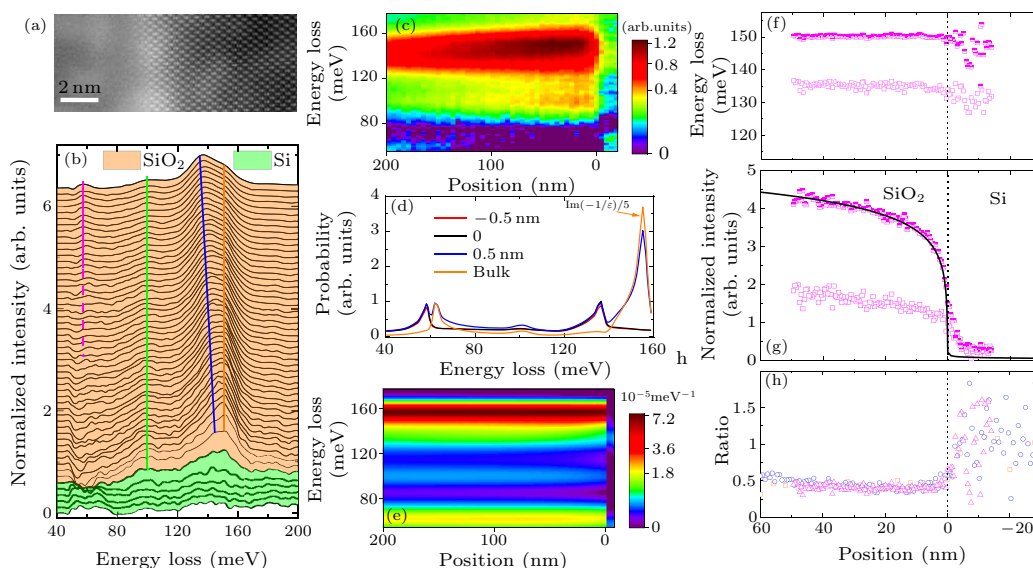

Fig. 4. Lattice vibrations near the SiO$_2$/Si interface. (a) An atomically resolved HAADF image of a-SiO$_2$/Si viewed in cross section. (b) Line profile of the SiO$_2$ vibrational signal with 0.78 nm every stack. [(c), (e)] Two-dimensional plots of normalized intensity for experiments and simulations, respectively. The interface is set to be zero, and positive distance denotes that the beam is in the SiO$_2$. The color bar represents the normalized intensity. (d) Energy loss function based on dielectric theory. [(f), (g)] The energy and intensity of the TO$_{3-\text{bulk}}$ and TO$_{3-\text{interface+surface}}$ modes as a function of the probe position. The open and the half up-filled squares represent the TO$_{3-\text{bulk}}$ and TO$_{3-\text{interface+surface}}$ modes, respectively. (h) The intensity of TO$_{3-\text{interface+surface}}$ to TO$_{3-\text{bulk}}$ ratio. The colored data points represent three sets of data recorded from different samples.

In the following, we discuss the interface effects on the lattice vibrations. Figures 4(a) and 4(b) show the atomically resolved HAADF image of SiO$_2$/Si interface and the selected line profile of SiO$_2$ spectrum (4.7 nm every step) with non-uniform thickness. Figures 4(c) and 4(e) show the two-dimensional plots of the normalized intensity for experiments and simulations, respectively. Note that when the beam is located in the SiO$_2$ side, the acquired signal is mixed with the signals of SiO$_2$ (both surface mode and bulk mode) and SiO$_2$/Si interface mode. Figure 4(d) shows the simulated energy loss function near the SiO$_2$/Si interface, where the interface mode and bulk mode are predicted to be obtained. In principle, the simulations show that the pure signal of SiO$_2$/Si interface vibrational mode can be obtained by placing the electron beam in the Si substrate for long-range Coulomb interaction because the retardation effects mask any inherent vibrational signal of the Si substrate.[35] Unfortunately, the signal in Si side is too weak to be extracted, even after very long acquisition time.

The energy of surface vibration in thickness of 80 nm is 137 meV, similar to the interface vibration at 136 meV. Thus we decompose the signal between 120 meV and 160 meV into two Gaussian peaks as the TO$_{3-\text{bulk}}$ and TO$_{3-\text{surface+interface}}$ modes. Their energy, intensity and the intensity ratio of TO$_{3-\text{surface+interface}}$ to TO$_{3-\text{bulk}}$ are shown in

Figs. 4(f)–4(h), respectively. The energy of interface mode is 136 meV, which is expected from the energy loss function shown in Fig. 4(d). No significant energy shift of both the modes is observed in Fig. 4(f). The intensity of the TO_{3-bulk} mode reaches 70% of its maximum at 3 nm from the interface and the intensity of the $TO_{3-surface+interface}$ mode drops steeply to zero within ∼10 nm from the interface. The black solid line is the expected retarded signal intensity of the TO_{3-bulk} mode,[36] which well describes the experimental data in the SiO_2 side.

The weak vibrational signal in the Si side may be due to the surface oxide layers in Si substrate[35] or the diffused electron probe. From the intensity ratio profile in Fig. 4(h), the intensity ratio of $TO_{3-surface+interface}$ to TO_{3-bulk} in the SiO_2 side is almost a constant ∼0.5 rather than a bulge at the interface. This indicates that the contribution from the top and bottom surfaces to total intensity of $TO_{3-surface+interface}$ is likely to be dominated due to thin foil geometry. However, on the Si side, the value of ratio is significantly larger than that in the SiO_2 side evidenced from three sets of data in Fig. 4(h). This can be understood by the fact that in the Si side the intensity of the interface mode is dominated based on the simulation in Fig. 4(d). Thus, the residual signal in the Si side near the interface mainly represents the interface mode.

In summary, we have investigated the vibrational behavior of the SiO_2/Si surface and interface using STEM-EELS. With sub-10 meV energy resolution, three optical vibrational modes of ∼60 meV, ∼103 meV and 150 meV are recorded. We find that the vibrational energy of the surface modes is lower than that of the corresponding bulk modes, which is in good agreement with the local dielectric theory. The maximum intensity of the surface mode occurs at the edge of the surface and gradually decreases obeying the zero-order modified Bessel function of the second kind in vacuum.[33] Inside the SiO_2 film, the vibrational energy of bulk modes keeps constant while the energy of surface modes strongly depends on the thickness. Approaching the SiO_2/Si interface, a weakly excited interface mode response at ∼136 meV is obtained. All the vibrational signal drops sharply within a few nanometers from the interface on the SiO_2 side. Our experimental measurements of local vibrational properties of SiO_2/Si give useful clues for further understanding and controlling the properties of SiO_2/Si heterostructure via surface and interface treatments, particularly for nanometer sized devices.

References

[1] Ashcroft N W 1976 *Solid State Physics* (New York: Brooks Cole)

[2] Houchmandzadeh B, Lajzerowicz J and Salje E 1992 *J. Phys.: Condens. Matter* **4** 9779

[3] Xia F N, Wang H, Xiao D, Dubey M and Ramasubramaniam A 2014 *Nat. Photon.* **8** 899

[4] Maradudin A A and Oitmaa J 1969 *Solid State Commun.* **7** 1143

[5] Ibach H and Mills D L 1982 *Electron Energy Loss Spectroscopy and Surface Vibrations* (New York: Academic Press)

[6] Zhang S Y et al 2018 *Phys. Rev. B* **97** 035408

[7] Griffiths P R 1975 *Chemical Infrared Fourier Transform Spectroscopy* (New York: Wiley)

[8] Stuart B 2005 *Kirk-Othmer Encyclopedia of Chemical Technology* (New York: Wiley)

[9] Efremov E V, Ariese F and Gooijer C 2008 *Anal. Chim. Acta* **606** 119

[10] Steidtner J and Pettinger B 2008 *Phys. Rev. Lett.* **100** 236101

[11] Krivanek O L et al 2014 *Nature* **514** 209

[12] Lagos M J, Trügler A, Hohenester U and Batson P E 2017 *Nature* **543** 529

[13] Crozier P A, Aoki T and Liu Q 2016 *Ultramicroscopy* **169** 30

[14] Govyadinov A A et al 2017 *Nat. Commun.* **8** 95

[15] Hachtel J A, Lupini A R and Idrobo J C 2018 *Sci. Rep.* **8** 5637

[16] Hudak B M et al 2017 *Nat. Commun.* **8** 15316

[17] Idrobo J C et al 2018 *Phys. Rev. Lett.* **120** 095901

[18] Lagos M J and Batson P E 2018 *Nano Lett.* **18** 4556

[19] Dwyer C et al 2016 *Phys. Rev. Lett.* **117** 256101

[20] Hage F S et al 2018 *Sci. Adv.* **4** eaar7495

[21] Rez P et al 2016 *Nat. Commun.* **7** 10945

[22] Nicollian E H 1977 *J. Vac. Sci. Technol.* **14** 1112

[23] Kirton M J et al 1989 *Semicond. Sci. Technol.* **4** 1116

[24] Tu Y H and Tersoff J 2000 *Phys. Rev. Lett.* **84** 4393

[25] Kröger E 1968 *Z. Phys. A: Hadrons Nucl.* **216** 115

[26] Moreau P, Brun N, Walsh C A, Colliex C and Howie A 1997 *Phys. Rev. B* **56** 6774

[27] Hohenester U and Trügler A 2012 *Comput. Phys. Commun.* **183** 370

[28] Bates J B, Hendricks R W and Shaffer L B 1974 *J. Chem. Phys.* **61** 4163

[29] Innocenzi P 2003 *J. Non-Cryst. Solids* **316** 309

[30] Montero I, Galán L, Najmi O and Albella J M 1994 *Phys. Rev. B* **50** 4881

[31] Lagos M J et al 2018 *Microscopy* **67** i3

[32] Innocenzi P, Falcaro P, Grosso D and Babonneau F 2003 *J. Phys. Chem. B* **107** 4711

[33] Howie A 1983 *Ultramicroscopy* **11** 141

[34] Liu B Y et al 2018 *J. Chin. Electron. Microsc. Soc.* **5** 474 (in Chinese)

[35] Venkatraman K, Rez P, March K and Crozier P A 2018 *Microscopy* **67** i14

[36] Garcia-Molina R, Gras-Marti A, Howie A and Ritchie R H 1985 *J. Phys. C* **18** 5335

Supplementary Material:

Probing Lattice Vibrations at SiO₂/Si Surface and Interface with Nanometer Resolution

Yue-Hui Li(李跃辉)[1,2], Mei Wu(武媚)[1,2], Rui-Shi Qi(亓瑞时)[1], Ning Li(李宁)[1,2],

Yuan-Wei Sun(孙元伟)[1,2], Cheng-Long Shi(施成龙)[3], Xue-Tao Zhu(朱学涛)[4],

Jian-Dong Guo(郭建东)[4], Da-Peng Yu(俞大鹏)[2,5,6], Peng Gao(高鹏)[1,2,6*]

[1]International Center for Quantum Materials, Peking University, Beijing, 100871

[2]Electron Microscopy Laboratory, School of Physics, Peking University, Beijing, 100871

[3]Nion Co. 11511 NE 118Th Street, Kirkland, Washington State, 98034, USA

[4]Beijing National Laboratory for Condensed Matter Physics and Institute of Physics, Chinese

Academy of Sciences, Beijing 100190

[5]Shenzhen Key Laboratory of Quantum Science and Engineering, Shenzhen 518055, China

[6]Collaborative Innovation Centre of Quantum Matter, Beijing 100871

Y.H.L. and M.W. contributed equally to this work.

Email: p-gao@pku.edu.cn

Data acquisition In our experiments, we used a Nion UltraSTEM[TM] 200 microscope with both monochromator and the aberration corrector operating at 60kV. The beam convergence semi-angle was 15mrad and the collection semi-angle was 24.4 mrad with a 1 mm spectrometer entrance aperture. The typical energy resolution (half width of the full zero loss peak, ZLP) was 8 meV, the probe beam current was ~5-10 pA and the dispersion of per channel was 0.47 meV. The typical dwell time was 100-200 ms to obtain good signal-noise ration spectra. The specimen studied in this work was 300 nm amorphous SiO₂ (a-SiO₂) on Si substrate. The cross-section sample was prepared by traditional mechanical polishing. We acquired single spectrum from different regions, line scan spectra, and map spectra to resolve the spatially dependent vibrational properties.

Calibration and background subtraction To correct the energy shift, we shifted the maximum point of ZLP to zero for unsaturated ZLP and shifted the centroid of two energies whose intensity was 5% lower than its peak value for saturated ZLP. To obtain more precise information from the spectra, we fitted the background with power law $I(\Delta E) = A_0 \cdot \Delta E^{-r}$. Note that generally, the third-order exponential function provides a more accurate fit, but due to the high energy resolution (~8.3 meV), there is little benefit using the exponential function.[1]

Theoretical analysis To quantitatively interpret the experiments, calculation of the vibrational response was performed. There are many theories and models based on classical dielectric response or quantum mechanical exploration to explain nanometer confined vibrations.[2-5] Here we do calculations mainly based on a semiclassical relativistic local dielectric model developed by E. KROGER,[2] which considers the coupling of the upper and lower surface and gives rise to symmetric and asymmetric guided slab modes.

There are two reasons to choose Gaussian function to fit the peak rather than Lorentz function: (1), SiO_2 sample is amorphous; a dielectric function based on a modified Gaussian profile was used to reproduce the infrared reflectivity spectra of silicate glass;[6] (2), the probing function (ZLP) is approximated as Gaussian distribution. It should be noted that to get a better decomposition, a new background function was subtracted to make two sides of the $TO_{3\text{-bulk}} + TO_{3\text{-surface}}$ signal approach zero, where two fitting region (105meV~115meV, 175meV~195meV) was chosen.

We calculate film thickness through plasmon peak, using formula:

$$t = \lambda \ln \frac{I_{tot}}{I_{ZLP}}$$

where, I_{tot} is the sum of all counts in a spectrum containing main plasmon signal, I_{ZLP} is the sum of zero loss peak, λ is the electron mean free path, whose detailed expression can be obtained from Ref. [7].
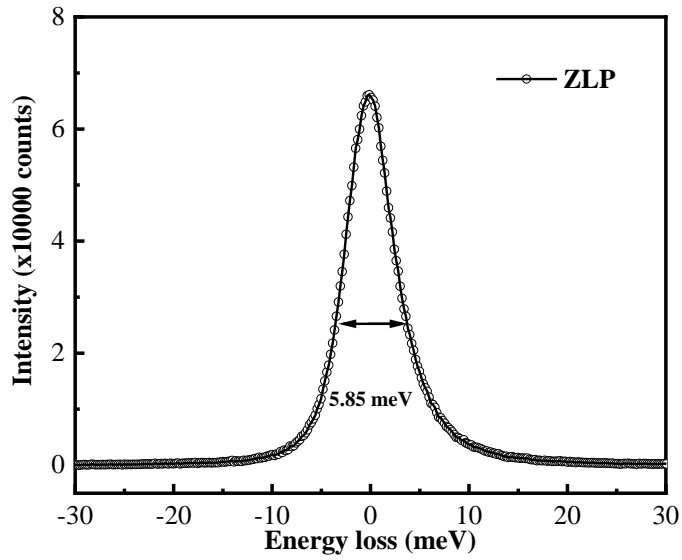
Fig. S1. The energy resolution is characterized by the FWHM of zero loss peak. The best energy resolution is ～ 6meV.
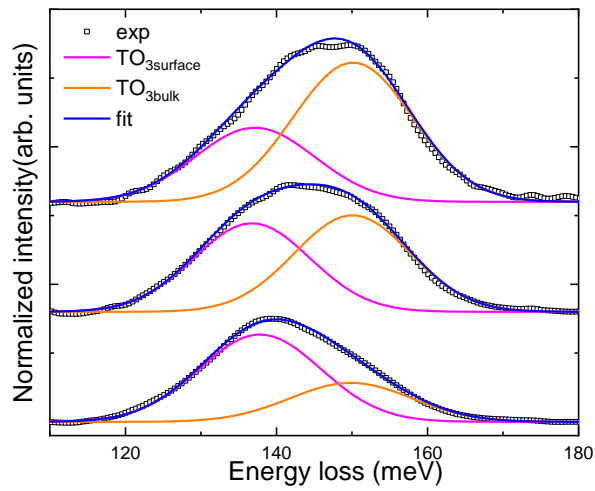

Fig. S2. Gaussian function to fit the peak. The black open square: experiment data; pink line: the fitted $TO_{3\text{-surface}}$ mode component; orange line: the fitted $TO_{3\text{-bulk}}$ mode component; blue line: sum of $TO_{3\text{-surface}}$ mode component and $TO_{3\text{-bulk}}$ mode component.

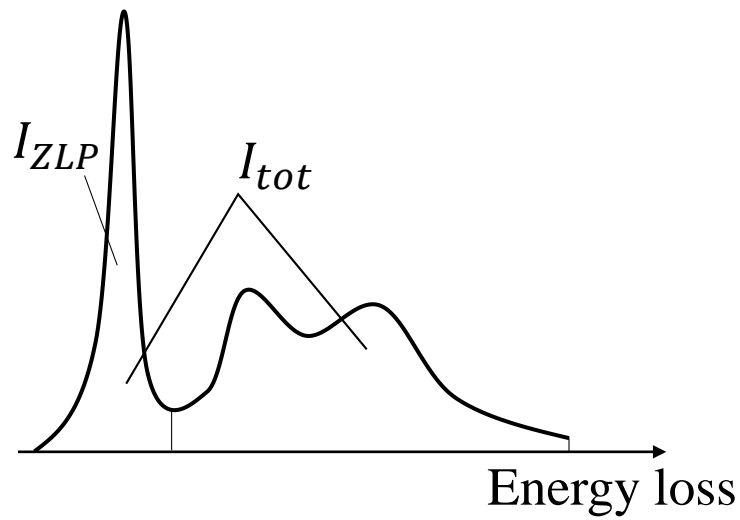**Fig. S3.** Sketch diagram of calculating thickness by log-ratio method.[7]

	#1	#2	#3	#4
TO_1	415	380	394	
TO_2	357	338	333	353
TO_3	259	276	242	251

Table 1. Decay constant b_0 (nm) for different vibrational modes. Different sets of data were fitted with exponential function $I = I_0 exp(-b/b_0)$.

References

[1] Hachtel J A, Lupini A R and Idrobo J C 2018 *Sci. Rep.* **8,** 5637

[2] Kröger E 1968 *Z. Für Phys. Hadrons Nucl.* **216,** 115–135

[3] Allen L J, Brown H G, Findlay S D and Forbes B D 2018 *Microscopy* **67,** i24–i29

[4] Howie A and Milne R H 1985 *Ultramicroscopy* **18,** 427–433

[5] Forbes B D and Allen L J 2016 *Phys. Rev. B* **94,** 014110

[6] De Sousa Meneses D, Malki M and Echegut P 2006 *J. Non-Cryst. Solids* **352,** 769–776

[7] Egerton R F 2011 *Electron Energy-Loss Spectroscopy in the Electron Microscope* (US: Springer)